Site-Specific Drug Delivery by Photochemical Internalization Enhances the Antitumor Effect of Bleomycin

Kristian Berg,[1] Andreas Dietze,[1,2] Olav Kaalhus,[1] and Anders Høgset[3]

Abstract

Purpose: Photochemical internalization is under development for improving macromolecular therapy by inducing photochemical damage to endocytic vesicles. This damage leads to the release of therapeutic macromolecules entrapped in endocytic vesicles into the cytosol. The macromolecules may in this way be able to interact with therapeutic targets instead of being degraded by lysosomal hydrolases. Bleomycin is used in several standard cancer chemotherapy regimens. Its hydrophilic and relatively large chemical structure limits its ability to penetrate membrane structures, which causes the accumulation of bleomycin in endocytic vesicles. The purpose of this study was to evaluate the therapeutic potential of aluminum phthalocyanine disulfonate ($AlPcS_{2a}$) – based photochemical delivery of bleomycin.

Experimental Design: Three tumors of different origin were grown s.c. in BALB/c (*nu*/*nu*) mice. The photosensitizer $AlPcS_{2a}$ and bleomycin were systemically administered and the tumor area was exposed to red light when the tumor volume had reached 100 mm^3. The tumor volume was measured frequently after treatment and the time for the tumor volume to reach 800 to 1,000 mm^3 was selected as the end point.

Results: The photochemical delivery of bleomycin induced a delayed tumor regrowth, and in two out of three tumor models, lead to 60% complete response, whereas no complete responses were seen after treatment with bleomycin alone. A statistical model to assess synergism was established. Combination of the photochemical treatment and bleomycin was found to induce a synergistic delay in tumor growth.

Conclusion: $AlPcS_{2a}$-based photochemical internalization of bleomycin induces a synergistic inhibition of tumor growth in three different tumor models. This treatment combination should be further considered for clinical utilization.

Chemotherapeutics requires efficient penetration into the cytosol of the target cells in order to reach their intracellular targets and exert their therapeutic activity. The need to enter the cytosol, e.g., through the plasma membrane, limits the exploitable chemical structure of chemotherapeutic agents to mostly small and lipophilic compounds penetrating the plasma membrane by passive diffusion. Some chemotherapeutic agents, such as bleomycin and cisplatin, exert a nonpermeant or semipermeant character (1, 2). The bleomycins are water-soluble glycopeptidic antibiotics (3). Their cytotoxicity is caused by inducing single- and double-stranded DNA breaks, resembling ionizing radiation with respect to type of DNA damage and repair (4). Bleomycin is used in standard cancer chemotherapies including treatment of squamous cell carcinomas of the head and neck, esophagus, bronchus, and skin, as well as testis cancer and malignant lymphomas. The sensitivity of tumor cells to bleomycin is highly variable due to its limited penetration through the plasma membrane. However, the cytotoxicity becomes similar and highly increased when the cytosol is exposed to similar amounts of bleomycin following electroporation (5). It has been estimated that as little as ~500 bleomycin molecules translocated to the cytoplasm may be sufficient to kill a cell (6). Thus, bleomycin may become a very efficient and specific chemotherapeutic agent by combination with a treatment modality activating its therapeutic potential only in the target tissue.

Photochemical internalization (PCI) is a new technology to improve the utilization of macromolecules in cancer therapy in a site-specific manner (7–9). The concept is based on the use of specially designed photosensitizers, which localize preferentially in the membranes of endocytic vesicles. Upon exposure to light of appropriate wavelengths, these photosensitizers induce the formation of reactive oxygen species of which singlet oxygen dominates. Similar photochemical reactions are the basis for photodynamic therapy (PDT), which is used for the treatment of many cancer indications as well as some noncancerous diseases (10). The photooxidation of the endocytic membranes leads to release of the contents of these vesicles into the cytosol. Macromolecules located in these vesicles will, in this way, reach the cytosol and be able to exert their biological activity instead of being degraded by lysosomal

Authors' Affiliations: Departments of [1]Radiation Biology and [2]Oncologic Surgery, the Norwegian Radium Hospital, Montebello, and [3]PCI Biotech AS, Oslo, Norway
Received 6/10/05; revised 8/10/05; accepted 8/29/05.

Grant support: Supported by the Norwegian Cancer Society and The Norwegian Radium Hospital Research Foundation.

The costs of publication of this article were defrayed in part by the payment of page charges. This article must therefore be hereby marked *advertisement* in accordance with 18 U.S.C. Section 1734 solely to indicate this fact.

Requests for reprints: Kristian Berg, Department of Radiation Biology, the Norwegian Radium Hospital, Montebello, N-0310 Oslo, Norway. Phone: 47-2293-4260; Fax: 47-2293-4270; E-mail: kristian.berg@labmed.uio.no.

doi:10.1158/1078-0432.CCR-05-1245

hydrolases. This PCI-based relocalization and activation of the macromolecules has the advantage of minimal side effects because the effect is localized to the irradiated area. In contrast to many other photochemical reactions, clinically relevant wavelengths in the red and even IR region may be used, allowing for a therapeutic effect in deeper layers of the target tissues. The endosomal escape of macromolecules such as genes, oligonucleotides, and proteins by means of PCI has been documented *in vitro* and *in vivo*, and has been shown to increase the therapeutic effect in a synergistic manner (7, 11–15). As in the case for macromolecules, bleomycin is practically nonpermeant to the plasma membrane and enters the cells by endocytosis whereby it may be degraded in the lysosomes; or due to the slow entrance into the cytosol, degraded by bleomycin hydrolase before reaching its therapeutic target in the nucleus. The aim of this study was to determine whether PCI could improve the therapeutic effect of bleomycin. In order to evaluate the general applicability of PCI for enhancing of the therapeutic effect of bleomycin, three different tumor models, a human colon adenocarcinoma, a human soft tissue sarcoma and a mouse colon cancer cell line, were used. The two most efficient photosensitizers for photochemical enhancement of the biological effect of macromolecule treatment have thus far been tetraphenylporphine disulfonate ($TPPS_{2a}$) and aluminum phthalocyanine disulfonate ($AlPcS_{2a}$; ref. 16). These photosensitizers, in combination with light, enhance the biological effect of proteins and genes to a similar extent *in vitro*, but due to the higher extinction coefficient of $AlPcS_{2a}$ in the wavelength region where light penetration through tissue is high (>600 nm) $AlPcS_{2a}$ is the preferred photosensitizer *in vivo*. In the present study, both photosensitizers were used, but only $AlPcS_{2a}$ was used for the *in vivo* studies. The results indicate that PCI of bleomycin induces a synergistic effect on tumor retardation in all the models.

Materials and Methods

Chemicals

$TPPS_{2a}$ and $AlPcS_{2a}$ with the sulfonate groups on adjacent phenyl and phthalate rings, respectively, were produced by Porphyrin Products (Logan, UT) and used as previously described (12, 17). 3-(4,5-Dimethylthiazol-2-yl)-2,5-diphenyltetrazolium bromide was purchased from Sigma (St. Louis, MO). Bleomycin (Lundbeck, Copenhagen, DK) was provided as a powder, 15 IU per vial according to the U.S. standard (15,000 IU according to the European Pharmacopoeia, 5.1) and was dissolved in 0.3 mL 0.9% NaCl. For *in vivo* use, further bleomycin dilutions (in 0.9% NaCl) were made to adjust the injection volume to 100 μL in all the cases.

Cell lines and tumor models

Cell culture. V79 Chinese hamster lung fibroblasts were grown as monolayers in MEM supplemented with 100 units/mL of penicillin, 100 μg/mL of streptomycin, and 10% FCS (Life Technologies, Scotland, United Kingdom). Cells of the line WiDr, derived from a human primary adenocarcinoma of the rectosigmoid colon (ATCC no. CCL-218), were subcultured in RPMI 1640 (Life Technologies) containing 10% FCS, 100 units/mL of penicillin, 100 μg/mL of streptomycin, and 2 mmol/L of L-glutamine.

Animals and tumor models. BALB/c (*nu/nu*) nude female mice were bred at the animal department of our institute. The mice were kept under specific pathogen–free conditions. Water and food was given ad libitum. All procedures involving mice were carried out in agreement with the protocols approved by the animal care committee at the Norwegian Radium Hospital, under control by the National Ethical Committee's guidelines on animal welfare. The mice were on average 20 to 25 g (5-8 weeks old) at the start of the experiments, and we used at least six mice per experiment group.

The WiDr human adenocarcinoma and the CT26 (CT26.CT25; ATCC no. CRL-2639) mouse colon carcinoma cells used in the present study were propagated by serial transplantation into the BALB/c (*nu/nu*) mice. The tumors are minced to homogeneity by a scalpel and 20 μL of the solution injected s.c. on the right hip of each mouse. A human malignant fibrous histiocytoma xenograft (TAX-1), established in 1988, was provided by Professor Ola Myklebost (Department of Tumor Biology, the Norwegian Radium Hospital, Oslo). It was derived from tissue obtained during resection after local relapse. The tissue was propagated by implantation of fragments (2 mm^3) in the left hind limb of nude mice (BALB/c *nu/nu*). The tumor size was measured two or three times per week by measuring two perpendicular diameters. Tumor volume was calculated using the following formula:

$$V = (W^2 \times L)/2$$

where W is the width and L the length diameters of the tumors measured. Animals were killed by cervical dislocation if the tumor volume reached 1,500 mm^3.

In vitro *treatment regimens.* The V79 cells were seeded into 12-well plates (75,000 cells/well, Costar, Corning, NY) and allowed to attach to the substratum for 6 hours. To some of the wells, 1 mL of medium with 0.7 μg/mL $TPPS_{2a}$ was added, and the cells were incubated for 18 hours. The cells were then washed thrice with medium. For the V79 cells treated with the "light after" procedure, the cells were then incubated in serum-containing medium for 4 hours with bleomycin or only for the last hour before exposure to light. Four hours after removal of $TPPS_{2a}$ the cells were illuminated as described below. After 3 days of incubation cell survival was measured by the 3-(4,5-dimethylthiazol-2-yl)-2,5-diphenyltetrazolium bromide assay (18). V79 cells treated with the "light before" approach were incubated in serum-containing medium for 4 hours after $TPPS_{2a}$ had been removed. The medium was removed, new medium added and the cells were illuminated as described below. Bleomycin was added immediately after the light treatment. After 1 or 4 hours of incubation with bleomycin, the cells were washed once with RPMI medium, 1 mL of medium added and after 3 days of incubation, cell survival was measured by the 3-(4,5-dimethylthiazol-2-yl)-2,5-diphenyltetrazolium bromide assay (18).

WiDr cells were seeded into 35 mm dishes (150×10^3 cells/dish, Falcon 3001, Becton Dickinson, Franklin Lakes, NJ) and allowed to attach for 48 hours. The medium was removed and the cells incubated with 1 mL serum-containing medium with 5 μg/mL $AlPcS_{2a}$ for 18 hours. The cells were washed thrice with medium and incubated in bleomycin-containing medium for 4 hours. The cells were washed once with RPMI medium, and after the addition of 1 mL drug-free medium, they were illuminated. After 3 days of incubation, cell survival was measured by the protein synthesis assay (17).

Light exposure. The V79 cells were exposed to light from a bank of four fluorescent tubes (Osram 18 W/67) with the highest fluence around 420 nm and a fluence rate of 11.7 mW/cm^2 (LumiSource, PCI Biotech, Oslo, Norway). The WiDr cells were exposed to red light from a bank of four fluorescent tubes (Philips TLD 15 W/950) filtered through a Roscoe 317 dark amber filter (LumiSource, PCI Biotech; fluence rate 1.5 mW/cm^2).

Treatment of xenografts. The stock solution of $AlPcS_{2a}$ was diluted to 1.25 mg/mL in PBS and ~200 μL was injected i.p. (final concentration 10 mg/kg) when the tumors had reached a size leading to tumor volumes of ~100 mm^3 at the day of illumination. Forty-eight hours after the injection of $AlPcS_{2a}$ 100 μL bleomycin (2, 5, or 15 IU/mL) was injected i.p. Thirty minutes after bleomycin injection, the tumors were illuminated as described below. The mice were randomly allocated to the different groups. Each animal got a unique number by marking the ears of the mice.

Light treatment. The tumors were illuminated with a 150 W halogen lamp (Xenophot HLX64640) filtered with a 580 nm long-pass and a 700 nm short-pass filter emitting 150 mW/cm^2. The animals were covered with aluminum foil except above the tumor area where a hole in the foil with a diameter 2 mm larger than the tumor diameter had been made.

Histologic analysis of lung tissue

In order to evaluate chronic inflammation and fibrosis in alveolar tissue, mice were sacrificed at the appropriate time points. The lung tissue was removed immediately by dissection and fixed in 4% formalin. Subsequently, the tissue were sectioned and staining was done with H&E, and detection of collagen was by van Gieson staining, in which collagen was imposed in red, nuclei in blue-black, and cytoplasma in yellow color (19). Histologic sections of 6 μm were examined microscopically to document the thickness of the alveolar wall and the extent of collagen deposition. Histologic analysis (H&E and collagen staining) were therefore done 2 to 6 weeks after treatment with PCI of 1,500 IU bleomycin, 1,500 IU and 3,000 IU bleomycin alone in mice with TAX-1 xenotransplants.

Statistics. The tumor growth data are subjected to survival analysis, using the day when the tumor volume supercedes the volume V_{crit} = 800 to 1,000 mm^3 (tumor model–dependent) as the failure time, and the duration of the experiment as the censoring time, if the tumor does not obtain this volume.

Because the failure times for groups with many failures seem to cluster around a specific average growth time, it is not feasible to compare the survival in the various groups by a Cox proportional hazard regression analysis. Instead, we use log-logistic survival function $S = 1/[1+ \exp(w)]$; where $w = (\ln t - \beta_0 - \beta_z)/\sigma$. β_0 is the logarithm of the median lifetime in the control, and σ determines the width of the failure region. β_z is a scalar product of a vector $z = \{z_1, z_2, z_3, \ldots\}$ indicating the kind of therapy 1, 2, 3,... used, and $\beta = \{\beta_1, \beta_2, \beta_3, \ldots\}$, the efficiency variables of the various therapies to be determined by the statistical calculation. In the present case, $z = \{0, 0, 0\}$ for the control, $\{1, 0, 0\}$ for bleomycin only, $\{0, 1, 0\}$ for PDT only, and $\{1, 1, 1\}$ for the combined therapies. In the latter case, $\beta_{add} = \beta_1 + \beta_2$ represents the additive effect of the combined therapies, whereas β_3 is the additional effect due to synergy.

We use an accelerated time model, i.e., changing the time scale by a factor of $\exp(-\beta_z)$, specific for each group, such that the survival curves of all groups coincide maximally after this transformation (see ref. 20). For those who are not familiar with this method, the formulas are cited in Appendix 1.

The present calculation scheme is related to the Cox proportional hazard regression, because the probability of failure within a time interval Δt is $-\Delta(\ln S) = \lambda(t;\beta_z)\,\Delta t \approx \lambda_0(t)\exp(-\beta_z)\,\Delta t$. Therefore, the proportional hazards method, corresponding to modifying the hazard function by $\exp(-\beta_z)$, i.e., $-\Delta(\ln S) = [\lambda_0(t)\exp(-\beta_z)]\,\Delta t$, should be equivalent to the time scaling method, $-\Delta(\ln S) = \lambda_0(t)\,[\exp(-\beta_z)\,\Delta t]$. In practice, the calculations will be very different.

Results

In vitro ***evaluation of photochemical activation of bleomycin.*** V79 cells were treated *in vitro* with various combinations and concentrations of bleomycin and $TPPS_{2a}$-PDT (Fig. 1A and B). Two treatment regimens were selected. In both regimens, the cells were initially treated overnight with $TPPS_{2a}$. In one

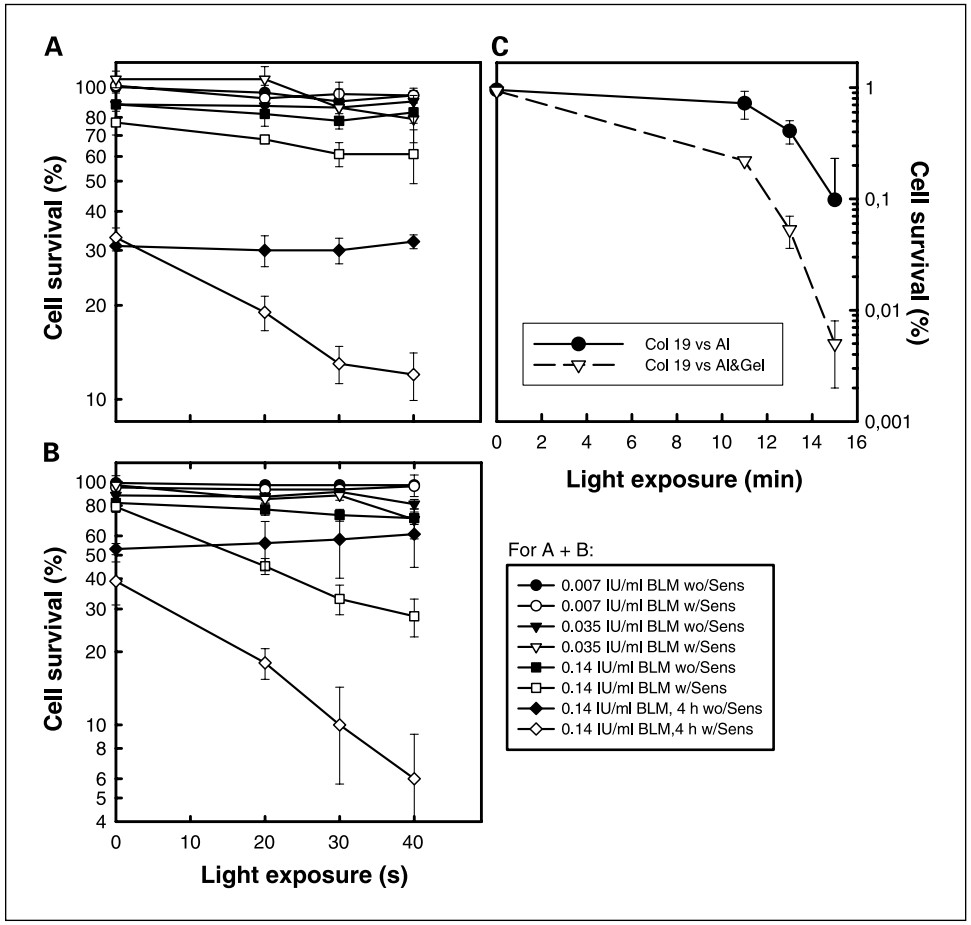

Fig. 1. Relative cell survival of V79 and WiDr cells treated with PCI of bleomycin. The V79 cells were treated with 0.7 μg/mL $TPPS_{2a}$ and light, and 1 hour with bleomycin if not otherwise indicated prior to (*A*, light after) or after (*B*, light before) the exposure of the cells to light as described in Materials and Methods. The cells were exposed to light in the presence (w/Sens) or absence (wo/Sens) of the photosensitizer $TPPS_{2a}$. The WiDr cells (*C*) were treated with 5 μg/mL $AlPcS_{2a}$ and light, and 4 hours with 0.14 IU/mL bleomycin prior to the exposure of the cells to light as described in Materials and Methods. Points, mean from three parallels; bars, SE.

regimen (light after), the cells were treated with bleomycin after the $TPPS_{2a}$ treatment, but before light exposure. In the other regimen (light before), the cells were treated with bleomycin immediately after exposure to light. It has previously been shown that both regimens may induce a similarly synergistic enhancement of the biological activity of selected macromolecules (21). PDT in combination with the lowest doses of bleomycin (0.007-0.035 IU/mL bleomycin, 1 hour) did not induce any cytotoxic effect in either of the treatment regimens. However, at a higher dose of bleomycin (0.14 IU/mL, 4 hours), inducing 30% to 50% cell inactivation by itself, the photochemical treatment reduced cell survival significantly. There were no differences in treatment effect between the two treatment regimens, although the "light before" regimen might be slightly more efficient at an intermediate bleomycin dose (0.14 IU/mL, 1 hour). It should be noted that the photochemical treatment alone did not induce any cytotoxicity. The cell survival in bleomycin-treated cells was not influenced by the light exposure in the absence of the photosensitizer.

Photochemical enhancement of the cytotoxic effect of bleomycin was also seen in the human WiDr adenocarcinoma cells (Fig. 1C). The WiDr cells were less sensitive to bleomycin treatment than the V79 cells and 4 hours of treatment with 0.14 IU/mL bleomycin did not induce any cytotoxicity in WiDr cells, whereas this treatment killed 30% to 50% of V79 cells. However, bleomycin reduced cell survival ~10-fold in photochemically treated WiDr cells. These results indicate that PCI has the potential to enhance the cytotoxicity of bleomycin treatment and warrants further *in vivo* evaluation.

In vivo evaluation of photochemical activation of bleomycin

WiDr tumor model. Photochemical activation of bleomycin was evaluated initially in s.c. growing human WiDr adenocarcinoma tumors. The photosensitizer $AlPcS_{2a}$ and bleomycin were administered systemically (i.p. 48 hours and 30 minutes prior to light exposure, respectively) followed by exposure to 145 J/cm^2 red light from a noncollimated light source. The time for the tumors to reach 800 mm^3 was selected as the end point.

The response to bleomycin and light in the absence of $AlPcS_{2a}$ in comparison to various controls is shown in Fig. 2A. The mean time for the tumors to reach the end point (Table 1) and statistical analyses (Table 2) indicate that all the treatments with bleomycin and light delays tumor growth significantly. When these treatments were compared with group 1 (no treatment), the differences were only on the border of being significant (P = 0.05-0.075), but this was due to one animal in the control group (group 1) with complete regression that is seen as a spontaneous regression, which occurs sporadically in this model. However, if group 1 (control), group 2 (PBS + light), and group 6 ($AlPcS_{2a}$ alone) were pooled together as one control group, all the bleomycin treatments were significantly different from the controls ($P < 0.01$). The highest dose of bleomycin (1.5 IU) induced a significantly longer tumor growth delay as compared with the lowest dose (0.2 IU), but was not significantly different from treatment with 0.5 IU. Treatment groups 4 and 5 (0.5 versus 0.2 IU bleomycin, respectively) did not induce a significantly different response, although 0.5 IU bleomycin tended to induce a stronger delay in tumor growth than 0.2 IU bleomycin. There was no significant difference in mean regrowth time between the groups receiving bleomycin plus light and those receiving bleomycin plus $AlPcS_{2a}$ in the absence of light (Tables 1 and 2).

The response to the photochemical treatment in combination with 1.5 IU bleomycin is shown in Fig. 2B. It was found that 60% of the animals receiving the combined treatment were tumor-free 200 days after treatment, whereas only 10% were tumor-free after PDT. The statistical analyses (Table 2) show that the tumor growth kinetics after photochemical treatment in combination with 1.5 IU bleomycin was significantly different from that after PDT and the corresponding bleomycin groups 7 and 3. In three out of four animals with tumor recurrences, the animals were apparently tumor-free 3 to 4 weeks after the PCI treatment.

Because both the PDT and the bleomycin groups induced a delay in tumor growth, documentation of synergism requires more detailed analyses, as described in Materials and Methods and in Appendix 1. Because the survival curves for the control (no treatment), the $AlPcS_{2a}$ alone, and the PBS + light groups seem to overlap, and because the two latter groups should not be expected to induce any effect on tumor growth, the data from these groups were pooled together in a control group with variable β_0. The bleomycin (1.5 IU) group and the PDT group were given additional variables, β_1 and β_2, respectively. In the combined treatment (PCI), an additional interaction variable, β_3, was introduced. The β's are then found by maximizing the log-likelihood function for all the animals, and the SEs are computed by inverting the information matrix.

To obtain the survival variable β_{12} for the combined bleomycin and PDT treatment if these were mutually independent, we add the individual survival variables, $\beta_{12} = \beta_1 + \beta_2$, corresponding to a contracted time scale $t^* = t\ \exp(-\beta_1 - \beta_2)$. The additional interaction variable, β_3, is then taken to yield a quantitative measure of synergy in the combined treatment.

The variable values found by the method described above are listed in Table 3. The present model seems to give a good fit to the experimental Kaplan-Meier survival curves, even if the width variable σ is common for all the survival curves, and was not only fitted to the control curve (data not shown). The significance levels between the various variables are in approximate agreement with the corresponding log-rank tests of the Kaplan-Meier survival curves.

The interaction variable, β_3, is positive and significantly different from zero, which indicates that there is a significant synergy effect in the combined treatment. This effect is quite large, $R = \beta_3/(\beta_1 + \beta_2) \approx 0.53$. In other words, the synergy effect is of the same order of magnitude as each of the effects of the two treatments combined.

A crude approximation for the purely additive bleomycin/PDT combined treatment survival curve can be obtained by time scaling the bleomycin-only treatment observation times multiplied by the ratio of the PDT and control median survival times, and vice versa (Fig. 2E). The resulting survival curve is in good agreement with the corresponding regression curve, and decreases significantly below the Kaplan-Meier survival curve for the PCI treatment, as found by the log rank test ($P \approx 0.01$).

The response to PCI with 0.5 and 0.2 IU bleomycin is shown in Fig. 2C and D, respectively. Both PCI groups were significantly different from the PDT group (P = 0.012 and 0.051, respectively). The PCI groups were on the border of being significantly different from the bleomycin groups (P = 0.055-0.078 and P = 0.0082-0.12 for treatments with 0.5 and

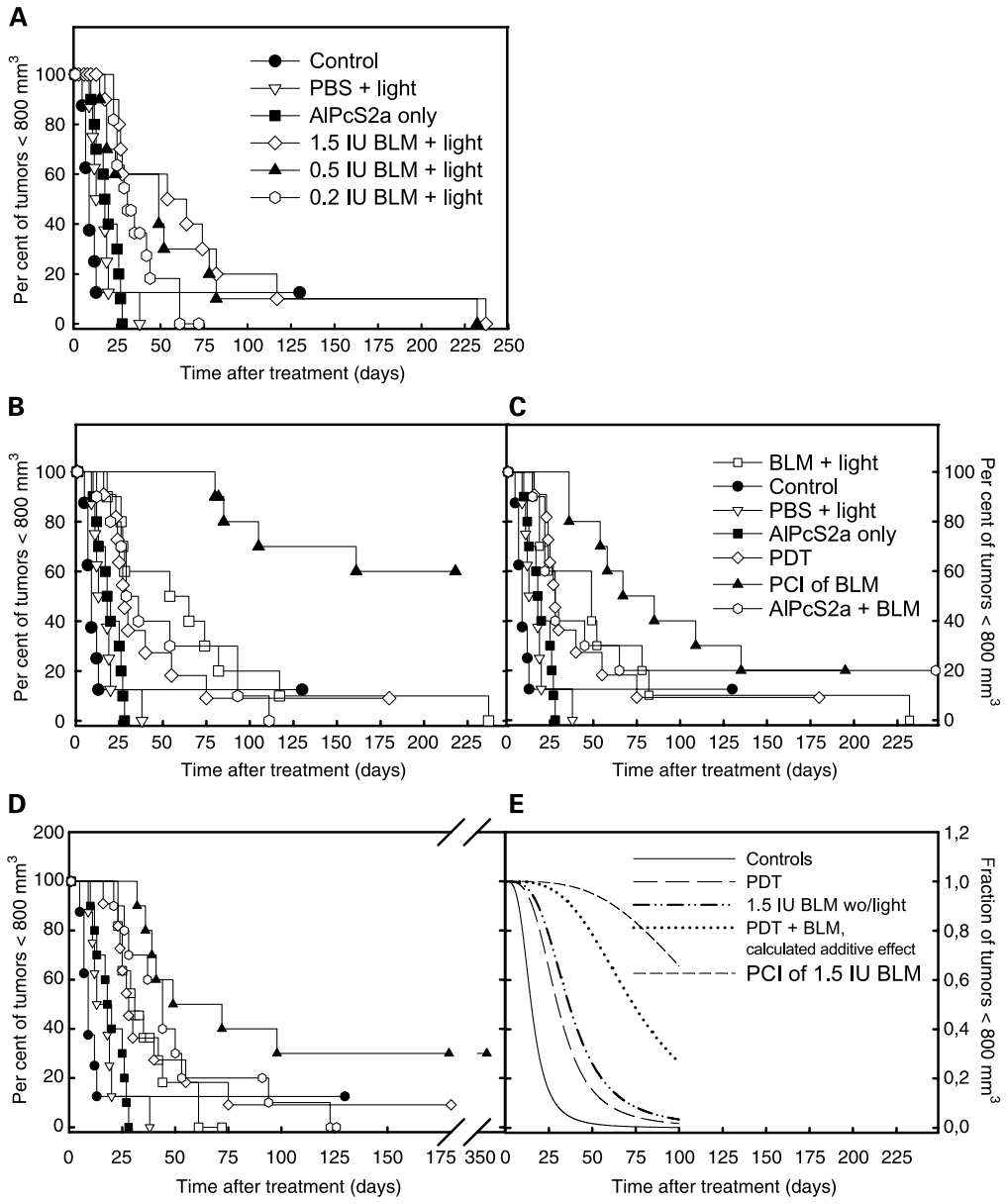

Fig. 2. Kaplan-Meier plots of response to treatment of WiDr tumors with bleomycin with and without in combination with photochemical treatment (PCI). *A*, the response to 0.2 to 1.5 IU bleomycin + light. The response to PCI of 1.5 IU (*B*), 0.5 IU (*C*), or 0.2 IU (*D*) bleomycin is shown with symbols in (*C*). The end point is the time after light exposure when the individual tumors have reached a tumor volume of 800 mm^3. The results are based on interpolations of the measured tumor volumes. *E*, a time-accelerated log-logistic survival of the data in (*B*) is presented. For clarity, all the data points are not shown. The controls (groups 1, 5, and 6; see Table 1) were pooled together. The calculated additive effect of combining PDT and 1.5 IU bleomycin as well as the results of PCI of 1.5 IU bleomycin is presented.

0.2 IU, respectively). Synergism could not be documented with PCI of 0.2 and 0.5 IU.

CT26 and TAX-1 tumor models. The evaluation of the possible synergistic delay in tumor growth by combining the $AlPcS_{2a}$-PDT and bleomycin treatments was also done on the mouse CT26 colon carcinoma and the human TAX-1 sarcoma models. On the basis of the results with the WiDr tumor model, only 1.5 IU bleomycin was administered to the animals.

The overall results are presented in a Kaplan-Meier plot in Fig. 3. The CT26 tumor model shows rapid growth kinetics with a mean time to reach 1,000 mm^3 of 7 days (Table 1). The tumors were exposed to 70 J/cm^2 of red light. The results show that both PDT and PCI of bleomycin induce a delay in tumor growth. The statistical analyses indicate that all the treatment groups were statistically different from each other despite none of the treatments inducing a complete response in any of the treatment regimens (data not shown). Table 1 indicates that the bleomycin treatment itself induced a slight (1.7 days), but significant, delay in tumor growth as compared with the controls. In comparison, PDT induced a more prolonged tumor growth delay of 5.8 days, whereas the combination (PDT + bleomycin, i.e., PCI) induced a delay in

Table 1. Mean time (days) for WiDr, CT26, and TAX-1 tumors to reach 800 to 1,000 mm^3 after the various treatments specified

Tumor model	Group	Treatment	No. of animals	Mean time to reach 800-1,000 mm^3*	SE
WiDr	1	untreated	8	24.0	14.2
	2	PBS + light	8	17.5	3.3
	3	1.5 IU bleomycin + light	10	72.8	20.7
	4	0.5 IU bleomycin + light	9	63.3	22.7
	5	0.2 IU bleomycin + light	11	36.3	4.3
	6	$AlPcS_{2a}$	10	19.6	2.1
	7	$AlPcS_{2a}$ + 1.5 IU bleomycin	10	50.3	11.3
	8	$AlPcS_{2a}$ + 0.5 IU bleomycin	11	75.4	30.8
	9	$AlPcS_{2a}$ + 0.2 IU bleomycin	10	52.0	10.2
	10	$AlPcS_{2a}$ + light (PDT)	11	47.6	13.5
	11	PCI of 1.5 IU bleomycin	10	173.9	18.3
	12	PCI of 0.5 IU bleomycin	10	112.9	19.0
	13	PCI of 0.2 IU bleomycin	10	142.6	44.0
CT26	1	growth control	12	7	0.28
	2	1.5 IU bleomycin	12	8.7	0.70
	3	PDT	9	12.8	0.36
	4	PCI of 1.5 IU bleomycin	12	19.4	0.60
TAX-1	1	growth control	9	14.8	0.81
	2	1.5 IU bleomycin $\pm$ light†	15	26.6	1.70
	3	PDT	10	44.0	8.36
	4	PCI of 1.5 IU bleomycin	5	96.0	14.6

*The mean time to reach 800 to 1000 mm^3 (800 mm^3 for WiDr tumors, 1000 mm^3 for CT 26 tumors and 900 mm^3 for TAX-1 tumors) is based on Kaplan-Meier survival analyses in SSPS where all animals in the groups are included.
† The 1.5 IU BLM and 1.5 IU BLM + light groups have been pooled together.

tumor growth of 12.4 days. In 8 out of 12 animals in the PCI group, the animals were apparently tumor-free for some period of time, i.e., from 2 to 3 days after light exposure and for the next 4 to 5 days, and in some cases up to about 2 weeks after PCI. The statistical analysis of possible synergism after PCI of bleomycin concluded that the combined treatments induced a clearly synergistic treatment effect ($P = 0.0014$).

Table 2. Statistical significance analyses (P) to reveal differences in therapeutic effect between various treatment regimens on the WiDr tumors

Treatment groups		Treatment groups											
	Treatment	1	2	3	4	5	6	7	8	9	10	11	12
1	untreated												
2	PBS + light	0.3632											
3	1.5 IU bleomycin + light	0.0528	0.0006										
4	0.5 IU bleomycin + light	0.0533	0.0046	0.4761									
5	0.2 IU bleomycin + light	0.0747	0.0011	0.0405	0.2500								
6	$AlPcS_{2a}$	0.2085	0.6978	0.0006	0.0175	0.0010							
7	$AlPcS_{2a}$ + 1.5 IU bleomycin	0.1185	0.047	0.4769	0.9393	0.2810	0.0014						
8	$AlPcS_{2a}$ + 0.5 IU bleomycin	0.0157	0.0016	0.8939	0.7598	0.6335	0.0103	0.9070					
9	$AlPcS_{2a}$ + 0.2 IU bleomycin	0.1125	0.0002	0.4661	0.8981	0.2047	0.0002	0.6942	0.9333				
10	$AlPcS_{2a}$ + light (PDT)	0.0502	0.0030	0.3373	0.6413	0.7995	0.0068	0.7178	0.9025	0.6435			
11	PCI of 1.5 IU bleomycin	0.0008	0.0000	0.0021	0.0012	0.0000	0.0000	0.0002	0.0053	0.0001	0.0003		
12	PCI of 0.5 IU bleomycin	0.0063	0.0000	0.1113	0.0548	0.0002	0.0000	0.0147	0.0777	0.0069	0.0123	0.1159	
13	PCI of 0.2 IU bleomycin	0.0125	0.0000	0.1983	0.1370	0.0082	0.0000	0.0728	0.0473	0.1192	0.0506	0.5926	0.5926

NOTE: The values are based on paired log-rank analyses of the time for the WiDr tumors to reach 800 mm^3.

Table 3. Results of the time-accelerated survival analysis in the log-logistic regression model for the treatments of WiDr tumors as presented in Fig. 4A, except that groups 1, 2, and 6 were pooled together

Treatment groups	$\beta_i \pm$ SE	Significance level (P)	Predicted median survival, days (range)
Control	2.69 ± 0.13	<0.001	14.7 (12.9-16.8)
Bleomycin	0.97 ± 0.26	<0.001 *	38.8 (29.0-51.9)
PDT	0.82 ± 0.23	<0.001 *	33.4 (24.9-44.8)
Bleomycin + PDT	1.79 ± 0.35	<0.001 *	88.2 (60.7-128)
Interaction	0.94 ± 0.41	0.02 †	226 (130-393)
Width (σ)	0.38 ± 0.05	<0.001	

NOTE: The animals were treated with 1.5 IU bleomycin. The bleomycin + PDT group is the theoretical calculation of an additive effect of combining the treatment regimens. The interaction group (β_3) indicates the supra-additive effect observed experimentally.
*Compared with control.
†Compared with treated groups.

Kaplan-Meier plots of the response of the TAX-1 tumors to the various treatment regimens are shown in Fig. 3B. It was found that bleomycin and PDT induced a significant delay in tumor growth of 12 and 30 days (Table 1), respectively, and with one exception in the PDT group, no complete responders (Fig. 3B). In contrast, 60% of the tumors were able to recover in the PCI group and the mean delay in growth was ~80 days (Table 1). The bleomycin and bleomycin plus light groups were not statistically different with respect to tumor growth. When these two groups were pooled together, all the treatments induced significantly different effects on tumor growth ($P < 0.016$). PCI of bleomycin induced a synergistic effect on tumor growth ($P = 0.020$).

Pulmonary fibrosis and weight loss. The major side effect of bleomycin treatment is pneumonitis that may progress into pulmonary fibrosis (22). Histologic analyses (H&E and collagen staining) were therefore done 2 to 6 weeks after treatment with PCI of 1.5 IU bleomycin, 1.5 and 3 IU bleomycin alone in mice with TAX-1 xenotransplants. However, no signs of pulmonary fibrosis or increased collagen formation were observed after any of these treatment regimens.

Weight loss is frequently observed in preclinical studies and clinically in combination therapies where bleomycin is included (23–25). Untransplanted mice treated with 1.5 IU bleomycin lost ~5% weight shortly after treatment, but regenerated weight within a few days (Fig. 4). TAX-1-transplanted mice treated with PCI of 1.5 IU bleomycin lost the same amount of weight as by bleomycin treatment alone, but needed somewhat more time to resume weight. The weights of the animals were similar in all treatment regimens (23.6-24.8 g) at the time of treatment.

Discussion

In view of previous findings that indicated enhanced activity of therapeutic and reporter macromolecules in cells exposed to PCI, we tested the efficacy of PCI in improving the ability of bleomycin to destroy tumors *in vitro* and *in vivo*. In all three tumors, separate implementation of the photochemical treatment (PDT) or bleomycin chemotherapy only slightly delayed tumor growth and induced no complete responses. However, the combination of PDT and bleomycin, i.e., PCI of bleomycin, not only further delayed the tumor growth, but also resulted in cure of 60% of the animals with subcutaneously growing WiDr and TAX-1 tumors. The statistical analyses indicate a synergistic effect of combining the two treatment regimens. In the mouse colon carcinoma line CT26, PCI of bleomycin did not induce a curative effect, but the delay in tumor growth was significantly longer than expected from combining the tumor responses from PDT and bleomycin separately, i.e., a synergistic effect was obtained. A similar therapeutic effect of PCI of bleomycin in all three tumor models indicates that this combination therapy has general applicability.

The cytotoxic effect of bleomycin varies widely between different tumors as well as between different organs. This is suggested to be due to differences in the cells' DNA repair capacity, bleomycin hydrolase activity, cellular uptake mechanisms, and possibly the rate of bleomycin efflux (26). The mechanisms of cellular uptake of bleomycin is not fully revealed, but as pointed out above, bleomycin is relatively large (molecular weight of about 1.5 kDa), hydrophilic, and is most likely able to diffuse across the plasma membrane to a limited extent only. Studies with human cells and Chinese hamster fibroblasts indicate that bleomycin binds to a 250 kDa receptor on the plasma membrane and is endocytosed in a receptor-mediated manner (5). The importance of the limited cellular uptake of bleomycin for its therapeutic effect has been documented by means of electroporation, where electric pulses induce a transient and reversible permeabilization of the cell membrane. The cytotoxicity of bleomycin may be enhanced a hundred-fold by means of electroporation and cell line differences may be attenuated by the electroporation technique (5, 6). The documented receptor-mediated endocytosis of bleomycin and therapeutic enhancement obtained by electroporation indicate that bleomycin is primarily entering the cells through endocytosis where bleomycin may be degraded by hydrolytic enzymes in late endosomes and lysosomes. The synergistic effect of combining a treatment modality rupturing endocytic vesicles with bleomycin treatment may therefore be explained by the transport mechanisms of bleomycin. Alternative explanations, such as photochemical inactivation of bleomycin hydrolase, however, cannot be excluded from its involvement in the photochemical enhancement of bleomycin activity.

In this study, bleomycin was systemically administered 30 minutes prior to the photochemical treatment. The half-life of

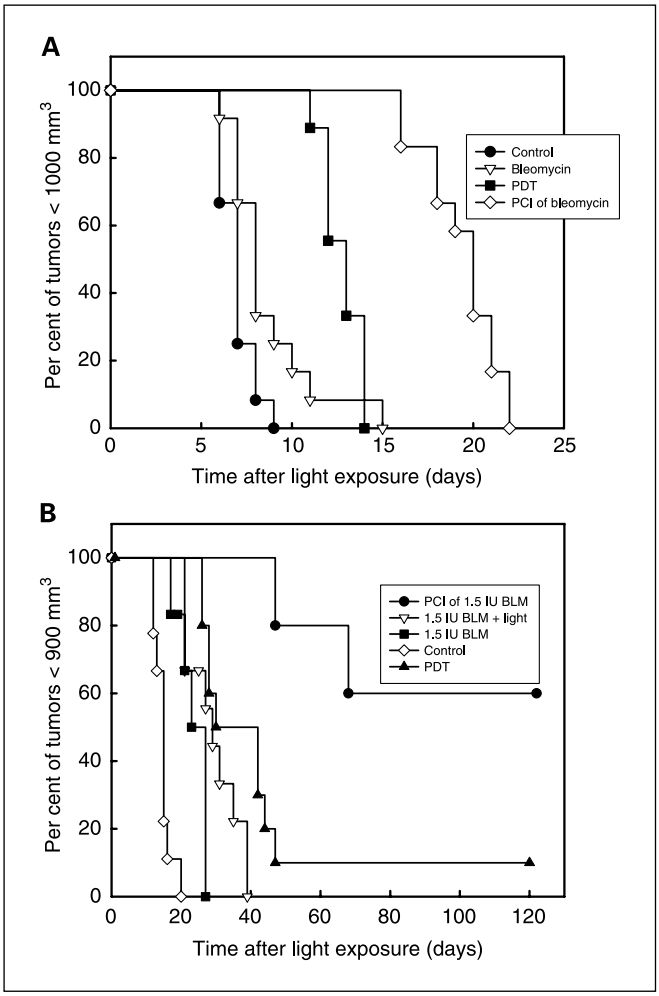

Fig. 3. Kaplan-Meier plots of responses to treatment of CT26 and TAX-1 tumors with 1.5 IU bleomycin with and without combination with photochemical treatment as indicated on the figure and in Table 1. The CT26 and TAX-1 tumors were exposed to 70 and 145 J/cm^2 of light, respectively. The end point is the time after light exposure when the individual tumors have reached a tumor volume of 1,000 or 900 mm^3 for the CT26 (*A*) and TAX-1 (*B*) tumors, respectively. The results are based on interpolations of the measured tumor volumes. For clarity, all the data points are not shown.

bleomycin in the blood of humans after i.v. injection is ~2 hours and ~70% of the bleomycin is excreted within the first 24 hours (27–29). In mice, the blood clearance time is much shorter and the amount of bleomycin in the tumor is practically unchanged from shortly after i.v. injection and for the following 24 hours (28). Because the *in vitro* data indicated that the photochemical treatment could be delivered prior to the bleomycin treatment, bleomycin administration shortly before exposure of the tumors to light was selected. This was based on the rapid redistribution of bleomycin from the blood circulation and the assumption that the "light before" regimen also occurs *in vivo*. This hypothesis was strengthened by previous studies with PCI of gelonin that showed similar therapeutic effects *in vivo* when gelonin was administered intratumorally 6 hours prior to light and immediately after light (12).[4] The timing between bleomycin administration and light exposure might, however, not be optimal in the present study. In patients, other factors such as renal function influence the pharmacokinetics of bleomycin (27) and should also to be taken into consideration in a clinical setting.

Treatment with bleomycin or PDT alone induced only a delay in tumor growth, and in general, the tumors were observable at all time points after treatment. However, all the tumors treated with PCI of 1.5 IU responded strongly to the treatment and a permanent cure or a period of apparent cure after treatment was observed in most of the tumor-bearing animals. During light exposure, the animals were covered with aluminum foil with a margin of about 2 mm to the visible tumor. This procedure is undertaken to avoid light exposure to normal tissue and especially the inner organs because light penetrates easily through the skin in athymic mice. In many cases, the tumor initiates regrowth in the border of the treatment area. The surviving tumor cells may therefore have escaped the light treatment. The injection of the tumor cells s.c. occurs at a low angle, almost horizontal, injection. The injection procedure might have lead to the deposition of a low number of tumor cells outside the area of light exposure. Some of the recurrences could therefore be due to the technical limitations of the experimental design.

The bleomycins contain several ring structures that may be oxidizable by PDT and thereby might be photochemically inactivated before reaching the nucleus, which is the main therapeutic target of bleomycin. The imidazole group in the metal-binding region is an obvious candidate for photooxidation by PDT because histidine is easily photooxidized. Based on studies of PDT-induced oxidation of purine and pyrimidine bases, the pyrimidine in the metal-binding region of bleomycin is expected to be oxidized by PDT only at high pH (30). However, the quantum yield of oxygen consumption during hematoporphyrin-based PDT is 0.049 (at pH 7.4) and the pyrimidine in bleomycin may therefore be photooxidized by

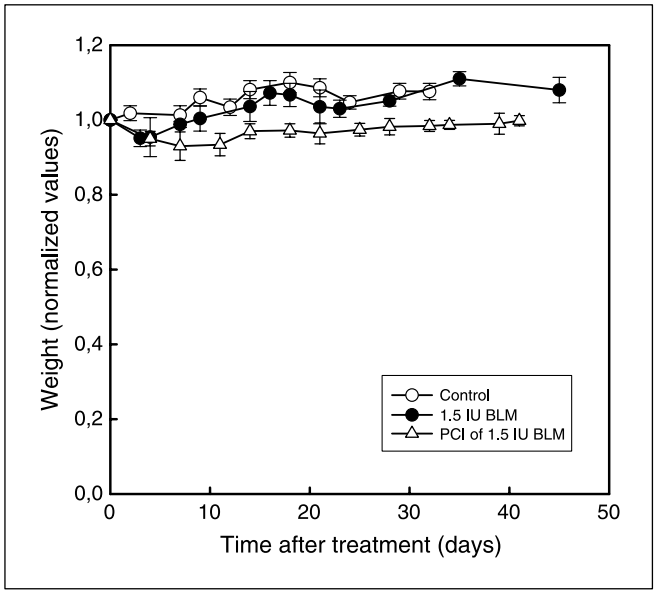

Fig. 4. The weight of the animals after treatment with bleomycin or PCI of bleomycin. The weight of the animals was measured after no treatment (controls), i.p. injection of 1.5 IU bleomycin, or PCI of 1.5 IU bleomycin as described in Materials and Methods. The weight is normalized for each animal to the weight at the day of bleomycin treatment or at a similar weight in the case of controls. Points, mean of three to eight animals; bars, SD.

[4] K. Berg and A. Høgset, unpublished data.

PDT. PDT has also been shown to oxidize 2,4,5-triphenylthiazole with methylene blue– and rose bengal–based PDT (31). Photodynamic oxidation of bleomycin may therefore attenuate the therapeutic effect of this combination therapy. It was recently found that the photochemical treatment might be executed prior to the delivery of the macromolecule (21). This is suggested to be due to the fusion of macromolecule-containing endocytic vesicles formed after the photochemical treatment with previously photooxidized vesicles. The *in vitro* results with PCI of bleomycin delivered prior to and after light activation showed similar enhancement of the bleomycin cytotoxicity. This argues against a significant oxidation of bleomycin by means of $TPPS_{2a}$-based PCI and could be explained by the localization of $TPPS_{2a}$ (and $AlPcS_{2a}$) mainly in membranes of the endocytic vesicle and the short range of action of singlet oxygen (32), the main reactive oxygen species formed after PDT. In contrast, photosensitizers that are located in the matrix of endocytic vesicles, such as $TPPS_4$, do not induce a PCI-mediated macromolecule activation when the cells are illuminated after the delivery of the macromolecule (16). However, when $TPPS_4$-based PCI is executed with the "light before" procedure, the biological activity of macromolecules can be significantly enhanced. Thus, photooxidation of bleomycin may occur under appropriate conditions, but does not seem to be of importance in $TPPS_{2a}$-based PCI.

The development of pneumonitis is the most severe side effect of bleomycin and occurs in up to 46% of all patients (26). In 3% of all patients, a fatal lung fibrosis develops, probably due to the low level of bleomycin hydrolase activity in the lung tissue. The toxic effects of bleomycin are suggested to be due to the direct effects of reactive oxygen species formed by bleomycin on the lung tissue and by immunologic reactions to the treatment. The importance of the thymus has been debated. Szapiel and coworkers reported that induction of pulmonary fibrosis was unaffected by the absence of thymus in mice (33), whereas other biochemical analyses and the use of inhibitors of immune function, such as steroids, as well as thymectomy, indicate that T cell depletion attenuate the induction of pulmonary fibrosis (34, 35). Histologic analysis of lung tissue did not reveal any fibrosis or collagen formation after PCI of bleomycin. However, this possible side effect needs special attention in the future development of PCI of bleomycin. The induction of pneumonitis and fibrosis is dose-dependent and correlates with the total accumulated dose (22). The strong and synergistic tumor response to PCI of bleomycin indicate that with PCI, the use of bleomycin might be limited to one or a few treatment sessions, thereby possibly reducing the total accumulated dose needed for achieving proper therapeutic responses.

The treatment with 1.5 IU bleomycin caused a reversible weight loss, which was somewhat more prolonged when combined with the photochemical treatment. In patient treatment, bleomycin is usually administered two to three times per week or continuously at a low dose for several days. The therapeutic response of PCI of bleomycin indicates that the treatment regimen may be substantially reduced as compared with existing standard treatment regimens and even only one treatment session may be sufficient for good therapeutic response. A rapidly reversible and mild weight loss should therefore not be of any major concern.

In conclusion, PCI of bleomycin has been shown to induce synergistic effects leading to both recovery and to delay in tumor progression in three different tumor models. The results warrant further development of this treatment regimen with respect to optimization of the treatment variables, but also indicate a clinical potential of the PCI technology on an approved chemotherapeutic agent.

Appendix 1

Modifying the presentation given in ref. (20), we have a log-likelihood function in the log-logistic regression model:

$\ln L(\beta_0, \beta, \sigma) = \sum_{1}^{n} lnL_i(w_i)$, where $L_i(w_i) = exp\ (w_i) / [1+ exp\ (w_i)]^2$ if individual i is a failure, and $L_i(w_i) = 1 / [1+ exp(w_i)]$ if individual i is a nonfailure (censored), summing over all individuals n. The variable $w_i = (lnt_i - \beta_0 - \boldsymbol{\beta_{zi}}) / \sigma$, where t_i is the time to failure, and $z_i = \{z_1, z_2, z_3, \ldots\}$ is the therapy indicator of individual i. The variables $\beta_0, \boldsymbol{\beta} = \{\beta_1, \beta_2, \beta_3, \ldots\}$ and and σ are determined by varying them until maximum of the log likelihood function is achieved. At this point in parameter space, all first derivatives of ln L with respect to these variables should be 0.

The approximate uncertainties in the parameter values can be found by computing the observed information matrix I (β_0, $\boldsymbol{\beta}$, σ), inverting it into the variance matrix V (β_0, $\boldsymbol{\beta}$, σ), and taking the square roots of the diagonal elements of the latter. The observed information matrix consists of second derivatives of the log-likelihood function with respect to the variables:

$$-\partial^2 lnL/\partial{\beta_0}^2 = \sigma^{-2}\Sigma A_i, -\partial^2 lnL/\partial\beta_0\partial\beta_u$$
$$= \sigma^{-2}\Sigma Z_{ui}A_i, -\partial^2 lnL/\partial\beta_u\partial\beta_v = \sigma^{-2}\Sigma z_{ui}z_{vi}A_i, -\partial^2 lnL/\partial\beta_0\partial\sigma$$
$$= \sigma^{-2}\Sigma w_i A_i, -\partial^2 lnL/\partial\beta_u\partial\sigma$$
$$= \sigma^{-2}\Sigma z_{ui}w_i A_i, -\partial^2 lnL/\partial\sigma^2 = \sigma^{-2}\Sigma {w_i}^2 A_i$$

where i refers to the individual as before, and u or v refers to the treatment type involved. In the present case, i.e., log-logistic regression, the common factor $A_i = 2\ exp(w_i) / [1 + exp(w_i)]^2$ if individual i is a failure, and half of this value otherwise.

Acknowledgments

We thank Bente Hovland, Marie-Therese Strand, and Hanne Mali Møllegård for skillful technical assistance. We also thank the Department of Tumor Biology for providing the TAX-1 tumor model.

References

1. Hyacinthe M, Jaroszeski MJ, Dang VV, et al. Electrically enhanced drug delivery for the treatment of soft tissue sarcoma. Cancer 1999;85:409–17.
2. Tozon N, Kodre V, Sersa G, Cemazar M. Effective treatment of perianal tumors in dogs with electrochemotherapy. Anticancer Res 2005;25:839–45.
3. Zaniboni A, Prabhu S, Audisio RA. Chemotherapy and anaesthetic drugs: too little is known. Lancet Oncol 2005;6:176–81.
4. Byfield JE, Lee YC, Tu L, Kulhanian F. Molecular interactions of the combined effects of bleomycin and X-rays on mammalian cell survival. Cancer Res 1976;36:1138–43.
5. Pron G, Mahrour N, Orlowski S, et al. Internalisation of the bleomycin molecules responsible for bleomycin toxicity: a receptor-mediated endocytosis mechanism. Biochem Pharmacol 1999;57:45–56.
6. Poddevin B, Orlowski S, Belehradek J, Jr., Mir LM. Very high cytotoxicity of bleomycin introduced into the cytosol of cells in culture. Biochem Pharmacol 1991;42 Suppl:S67–75.

7. Berg K, Selbo PK, Prasmickaite L, et al. Photochemical internalization: a novel technology for delivery of macromolecules into cytosol. Cancer Res 1999;59:1180–3.

8. Hogset A, Prasmickaite L, Selbo PK, et al. Photochemical internalisation in drug and gene delivery. Adv Drug Deliv Rev 2004;56:95–115.

9. Granville DJ, Levy JG, Hunt DW. Photodynamic therapy induces caspase-3 activation in HL-60 cells. Cell Death Differ 1997;4:623–8.

10. Brown SB, Brown EA, Walker I. The present and future role of photodynamic therapy in cancer treatment. Lancet Oncol 2004;5:497–508.

11. Dietze A, Peng Q, Selbo PK, et al. Enhanced photodynamic destruction of a transplantable fibrosarcoma using photochemical internalisation of gelonin. Br J Cancer 2005;92:2004–9.

12. Selbo PK, Sivam G, Fodstad O, Sandvig K, Berg K. *In vivo* documentation of photochemical internalization, a novel approach to site specific cancer therapy. Int J Cancer 2001;92:761–6.

13. Folini M, Berg K, Millo E, et al. Photochemical internalization of a peptide nucleic acid targeting the catalytic subunit of human telomerase. Cancer Res 2003;63:3490–4.

14. Hogset A, Ovstebo EB, Prasmickaite L, et al. Light-induced adenovirus gene transfer, an efficient and specific gene delivery technology for cancer gene therapy. Cancer Gene Ther 2002;9:365–71.

15. Morrow T. Barrett's esophagus seen in new photodynamic light. Manag Care 2003;12:44–5.

16. Prasmickaite L, Hogset A, Berg K. Evaluation of different photosensitizers for use in photochemical gene transfection. Photochem Photobiol 2001;73:388–95.

17. Selbo PK, Sivam G, Fodstad O, Sandvig K, Berg K. Photochemical internalisation increases the cytotoxic effect of the immunotoxin MOC31-gelonin. Int J Cancer 2000;87:853–9.

18. Hogset A, Prasmickaite L, Tjelle TE, Berg K. Photochemical transfection: a new technology for light-induced, site-directed gene delivery. Hum Gene Ther 2000;11:869–80.

19. Crury RAB, Wallington EA. Carleton's histological technique. 5th ed. Oxford: Oxford University Press; 1980.

20. Kalbfleisch JD, Prentice RL. The statistical analysis of failure time data. New York: John Wiley and Sons, Inc.; 1980.

21. Prasmickaite L, Hogset A, Selbo PK, et al. Photochemical disruption of endocytic vesicles before delivery of drugs: a new strategy for cancer therapy. Br J Cancer 2002;86:652–7.

22. Hay J, Shahzeidi S, Laurent G. Mechanisms of bleomycin-induced lung damage. Arch Toxicol 1991;65:81–94.

23. Gong LK, Li XH, Wang H, et al. Feitai attenuates bleomycin-induced pulmonary fibrosis in rats. Biol Pharm Bull 2004;27:634–40.

24. Posner MR, Weichselbaum RR, Fitzgerald TJ, et al. Treatment complications after sequential combination chemotherapy and radiotherapy with or without surgery in previously untreated squamous cell carcinoma of the head and neck. Int J Radiat Oncol Biol Phys 1985;11:1887–93.

25. Shankar Giri PG, Taylor SA. Concurrent chemotherapy and radiation therapy in advanced head and neck cancer. Am J Clin Oncol 1987;10:417–21.

26. Chen J, Stubbe J. Bleomycins: towards better therapeutics. Nat Rev Cancer 2005;5:102–12.

27. Crooke ST, Comis RL, Einhorn LH, et al. Effects of variations in renal function on the clinical pharmacology of bleomycin administered as an i.v. bolus. Cancer Treat Rep 1977;61:1631–6.

28. Oken MM, Crooke ST, Elson MK, Strong JE, Shafer RB. Pharmacokinetics of bleomycin after i.m. administration in man. Cancer Treat Rep 1981;65:485–9.

29. DeNardo GL, Krohn KA, DeNardo SJ. Comparison of oncophilic radiopharmaceuticals, *I-fibrinogen, 67Ga-citrate, 111In-bleomycin, and *I-bleomycin in tumor-bearing mice. Cancer 1977;40:2923–9.

30. Dubbelman TMAR, Van Steveninck AL, Van Steveninck J. Hematoporphyrin-induced photo-oxidation and photodynamic cross-linking of nucleic acids and their constituents. Biochem Biophys Acta 1982;719:47–52.

31. Matsuura T, Saito I. Photoinduced reactions. XXXIV. Photosensitized oxygenation of 2,4,5-triphenylthiazole. Bull Chem Soc Japan 1969;42:2973–5.

32. Moan J, Berg K. The photodegradation of porphyrins in cells can be used to estimate the lifetime of singlet oxygen. Photochem Photobiol 1991;53:549–53.

33. Szapiel SV, Elson NA, Fulmer JD, Hunninghake GW, Crystal RG. Bleomycin-induced interstitial pulmonary disease in the nude, athymic mouse. Am Rev Respir Dis 1979;120:893–9.

34. Schrier DJ, Phan SH, McGarry BM. The effects of the nude (*nu/nu*) mutation on bleomycin-induced pulmonary fibrosis. A biochemical evaluation. Am Rev Respir Dis 1983;127:614–7.

35. Phan SH, Thrall RS, Williams C. Bleomycin-induced pulmonary fibrosis. Effects of steroid on lung collagen metabolism. Am Rev Respir Dis 1981;124:428–34.